Azimuthal dependence of the differential cross section in electron scattering from free oriented CH_3Cl molecules

M. Volkmer,[1] Ch. Meier,[1] J. Lieschke,[1] R. Dreier,[1] M. Fink,[2] and N. Böwering[1]

[1]*Fakultät für Physik, Universität Bielefeld, D-33501 Bielefeld, Germany*
[2]*Physics Department, The University of Texas at Austin, Austin, Texas 78712*

An azimuthal dependence for 1-keV electrons scattered elastically at a fixed polar angle from a beam of free, spatially oriented CH_3Cl molecules prepared by an electrostatic hexapole technique was observed. Pronounced azimuthal distributions with orientation-dependent contributions of several percent were measured, demonstrating that for preferentially perpendicular orientation of the molecules with respect to the electron beam the diffraction pattern is no longer cylindrically symmetrical and reflects directly the orientation and alignment of the scattering state ensemble. The data are compared with model calculations using the independent-atom model and hexapole transmission calculations of the focused rotational state mixtures, taking both the linear and the quadratic Stark effect into account. Inclusion of the second-order Stark effect changes the calculated azimuthal distributions significantly and improves the agreement between experiment and theory. [S1050-2947(97)50509-9]

PACS number(s): 34.80.Bm, 33.15.Dj, 39.10.+j

Electron scattering from molecules in the gas phase [1–3] leads to a characteristic diffraction pattern of diffuse concentric interference rings. It can be analyzed by fitting procedures to obtain information on the molecular structure. The differential cross section has cylindrical symmetry around the electron beam direction since the distribution of the molecules is normally isotropic with no preferred axis orientation. In contrast, in low-energy electron diffraction from surface atoms and adsorbates (LEED), the diffraction pattern of elastically backscattered electrons exhibits a pronounced azimuthal dependence (LEED spots) that is analyzed to determine the surface topology. Similarly, if an orientation or alignment of free gas molecules can be introduced (at least partially) in a direction perpendicular to the incident electrons, the cylindrical symmetry is lifted, and it has been predicted that more detailed spatial information on the molecular structure (e.g., bond angles) will be obtainable. Here we report experimental results that show that an azimuthal dependence exists in electron scattering from a beam of free molecules oriented by means of the hexapole technique.

The novel characteristics and inherent advantages of the scattering from anisotropic gaseous targets have been discussed in several theoretical studies in recent years. While calculating the electron scattering for state-selected polar molecules, Allan and Dickinson first pointed out that there should be a pronounced azimuthal dependence of the differential cross section [4]. In their calculations in 1989, Fink and co-workers [5,6] obtained a strong angular dependence of the cross section for CH_3I molecules held fixed in space using the independent-atom model (IAM) [1–3]. Kohl and Shipsey developed this model further [7] and treated the scattering from oriented molecules in specific selected rotational states. They also discussed the advantages of the perpendicular over the parallel scattering geometry. Furthermore, they showed that the two-dimensional scattering pattern with both polar and azimuthal dependence can be inverted by a special two-dimensional Fourier transform to

obtain a real-space image of the molecule, independent of a model [8]. In the field of ultrafast electron diffraction from laser-aligned molecules, Williamson and Zewail have discussed the expected azimuthal dependence [9]. General theoretical formulas characterizing steric effects in electron-molecule scattering were given by Blum and co-workers, who presented numerical R-matrix results at 2- and 8-eV scattering energy for aligned N_2 [10].

In 1992 we reported the observation of additional molecular interference contributions in electron diffraction from free oriented molecules [11]. The dependence of the elastic-scattering cross sections on the polar angle was obtained for a continuous beam of CH_3I molecules, which were state-selected by an electrostatic hexapole and oriented in a weak homogeneous electric field. Subsequent studies with CH_3Cl [12] and CH_3I [13], also oriented preferentially parallel or antiparallel to the electron beam, showed oscillating deviations from the scattering pattern of unoriented molecules up to 4% as a function of momentum transfer, quite similar in shape to IAM calculations. Steric effects of similar magnitude were observed recently by two other groups in indirect [14] and direct [15] electron-impact ionization of CH_3Cl molecules with parallel and antiparallel orientation. However, due to the axial symmetry of this collision geometry there can be no dependence on the azimuthal angle in all these experiments. Since an azimuthal dependence of the diffraction pattern is a prerequisite for a two-dimensional structure analysis and since significantly different effects were predicted for preferentially perpendicular electron-molecule collisions [7], we have modified our apparatus to record the orientational interference pattern in the perpendicular scattering geometry. Here, we discuss our first results for CH_3Cl obtained in this configuration.

The apparatus has been described in detail before [11,13]; only the essential features and necessary modifications will be outlined here. A continuous supersonic beam of CH_3Cl (stagnation pressure, 1850 mbar; rotational temperature,
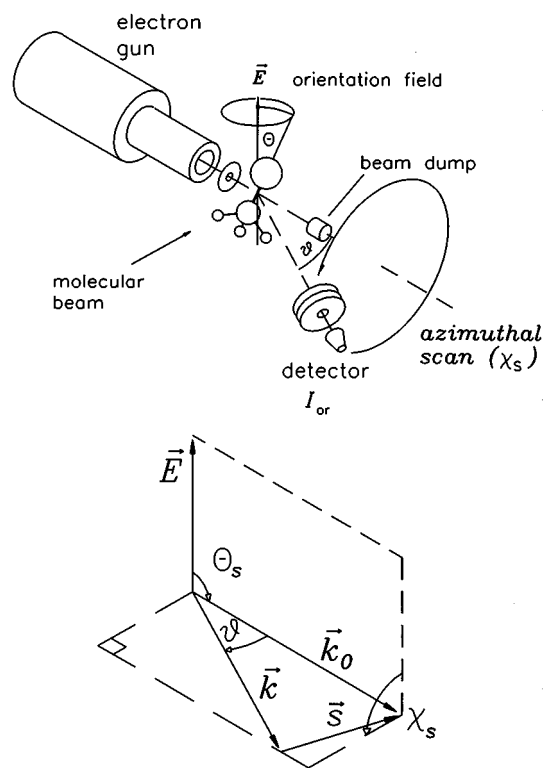
FIG. 1. Upper part: geometric arrangement for measurements of the azimuthal scattering distributions for molecules oriented preferentially perpendicularly to the electron beam. The lower diagram illustrates the relevant vectors and angles in this scattering geometry.

$T_{rot} \sim 25$ K) [12] is partially state-selected and focused by a hexapole field through a guiding field into the orientation field region where the scattering takes place (cf. Fig. 2 of Ref. [11]). Depending on the hexapole voltage U_0, different molecular state ensembles with different orientational axis distributions reach the scattering region. Using an electron beam of 1-keV electron energy and ca. 8-μA current, the intensity of the electronically elastic scattering is recorded by a rotatable detector consisting of a retarding field analyzer and a channeltron. To achieve a preferentially perpendicular orientation of the molecular symmetry axis with respect to the incident electrons, a different guiding and orientation field plate arrangement (10-mm plate distance), rotated by 90° around the molecular beam direction compared to the previous one, was used inside a grounded metallic frame shielding the scattering region (entrance hole, 6-mm diameter; exit slit, 12-mm height, 100-mm length).

The detector (effective acceptance angles: ±0.5° polar, ±1° azimuthal) was mounted off axis on a rotary motion feedthrough and carefully aligned. A beam dump for the undeflected electrons was attached to the rotation axis so that at a fixed polar scattering angle ϑ the electron-scattering distribution could be recorded on a circle covering the azimuthal angle from $\chi_s = 0°$ to $\chi_s = 360°$, see Fig. 1. χ_s describes the orientation of the scattering plane with respect to the electric-field vector $\vec{E}$. With this detection geometry the electron beam is slightly deflected when it passes through the perpendicular orientation field. This was compensated for with the deflection plates of the electron gun; also, the orientation

field strength in the scattering region was reduced to 20 V/cm. Even at 20 V/cm the degree of orientation for the $|111\rangle$ state of CH_3Cl was not substantially lowered, see Refs. [14–16].

By switching only the guiding field off, the orientation of the molecules can be turned off before they reach the scattering region, without any influence on the incident electron beam and the trajectories of the molecules. The scattering intensities $I_{or}^{\pm}(\chi_s, \vartheta)$ and $I_{unor}^{\pm}(\chi_s, \vartheta)$ for both oriented and unoriented molecules can be obtained. (The upper index $+$ or $-$ denotes an angle θ_s of 90° or 270°, respectively, between the orientation field $\vec{E}$ and the momentum of the incident electrons $\vec{k}_0$.) By taking intensity differences, the contributions from purely atomic scattering and from the molecular interference of unoriented molecules are eliminated, in contrast to the data analysis for unoriented molecules where the atomic contributions have always to be modeled [3]. The new orientation-dependent mean interference term $\bar{M}^{\pm}(\chi_s, \vartheta)$ for the focused molecular state ensemble can then be extracted directly as a fraction of the cross section for unoriented molecules, $\sigma_{unor} = (d\sigma/d\Omega)_{unor}$, according to [13]

$$\frac{\bar{M}^{\pm}(\chi_s, \vartheta)}{\sigma_{unor}} = \frac{I_{or}^{\pm}(\chi_s, \vartheta) - I_{unor}^{\pm}(\chi_s, \vartheta)}{I_{unor}^{\pm}(\chi_s, \vartheta)}. \quad (1)$$

Before Eq. (1) was applied the background count rates were subtracted from the scattering intensities, since a large fraction of the total count rate arises from residual gas scattering (vacuum pressure in the scattering chamber, $p \approx 3 \times 10^{-8}$ mbar). This background signal was determined by switching the hexapole off, since its central beam stop then effectively blocks the molecular beam and prevents it from reaching the scattering region.

Azimuthal distributions were recorded by rotating the detector in steps of 10° at fixed polar angle ϑ and given field orientation angle θ_s (90° or 270°). At each detector position four intensity measurements were made (by switching the guiding field on and off and the hexapole voltage on and off, respectively); the orientational interference terms were then determined as outlined above. By taking the intensity ratio of Eq. (1), residual eccentricities of the azimuthal scans (i.e., small azimuthal intensity variations in the scattering distributions for unoriented molecules, which should not exist for perfect cylindrical symmetry) are also eliminated. Each distribution shown below represents the average of many scans with a total data accumulation time of typically 2–3 h/point.

In contrast to the parallel and antiparallel scattering configuration, a reversal of the orientation field polarity does not provide any new information in the case of the perpendicular geometry, since $\bar{M}^{+}(\chi_s, \vartheta)$ is equal to $\bar{M}^{-}(\chi_s + 180°, \vartheta)$. The total orientational interference contribution can still be divided into pure alignment and pure orientation parts $\bar{M}_A$ and $\bar{M}_O$, representing even and odd interference terms, similarly as discussed previously [12,13]:

$$\bar{M}_A(\chi_s, \vartheta) = [\bar{M}^{+}(\chi_s, \vartheta) + \bar{M}^{+}(\chi_s - 180°, \vartheta)]/2, \quad (2)$$

$$\bar{M}_O(\chi_s, \vartheta) = [\bar{M}^{+}(\chi_s, \vartheta) - \bar{M}^{+}(\chi_s - 180°, \vartheta)]/2. \quad (3)$$
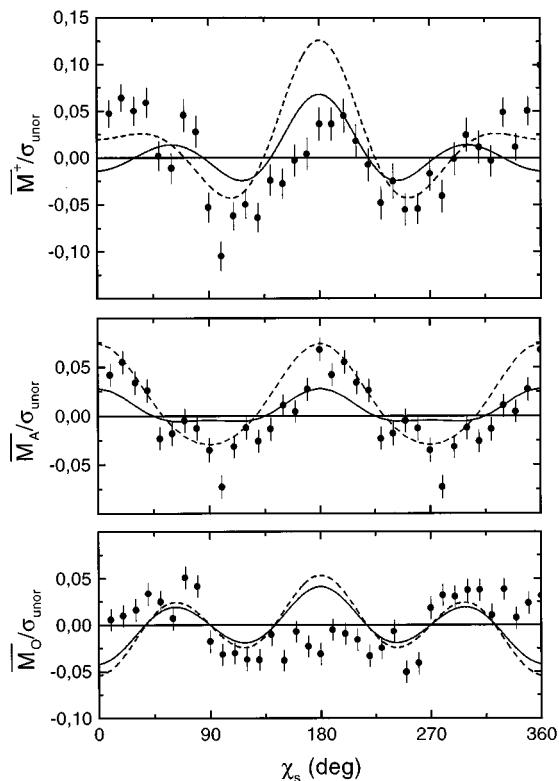
FIG. 2. Azimuthal dependence of the molecular orientational interference contributions $\bar{M}^+/\sigma_{unor}$, $\bar{M}_A/\sigma_{unor}$, and $\bar{M}_O/\sigma_{unor}$ obtained at a fixed polar angle of 8° for the oriented rotational state mixture focused at $U_0=\pm 4$ kV. Data points, experimental results; curves, IAM calculations using the linear Stark effect only (dashed lines) or the linear and quadratic Stark effect (full lines) to model the relative state populations.

Figures 2 and 3 show the results for $\bar{M}^+/\sigma_{unor}$, $\bar{M}_A/\sigma_{unor}$, and $\bar{M}_O/\sigma_{unor}$ obtained at a fixed polar angle (momentum transfer, $s=22.6$ nm^{-1}) for a hexapole rod voltage of $U_0=\pm 4$ kV and $U_0=\pm 10$ kV, respectively. The polar scattering angle was measured geometrically to be $8.0\pm 0.5°$, assuming that the molecular beam and the electron beam cross at the center of the orientation field. The orientational interference contributions represent several percent of the total cross section; they are generally larger than the corresponding oscillations found for the parallel geometry [12]. The distribution $\bar{M}^+/\sigma_{unor}$ is only symmetric with respect to $\chi_s=0°$ and $\chi_s=180°$ and has no symmetry with respect to $\chi_s=90°$ or $\chi_s=270°$; this reflects that there are also odd interference contributions $\bar{M}_O/\sigma_{unor}$ [shown in Figs. 2(c) and 3(c)]. In principle, this is different from the expected azimuthal distributions for the case of laser-prepared molecular scattering targets [9], since in the static electric field the molecular axis is not only aligned but, moreover, oriented in space.

Our data confirm the general trends, already found in the polar scattering distributions for $\theta_s=0°$ and $180°$ [12], that in the interference contributions even parts ($\bar{M}_A$) are generally larger than odd ones ($\bar{M}_O$); with respect to χ_s the total interference patterns reflect mainly the periodicity of the alignment contributions [Figs. 2(b) and 3(b)]. The differences in the results of Figs. 2 and 3 originate from the fact
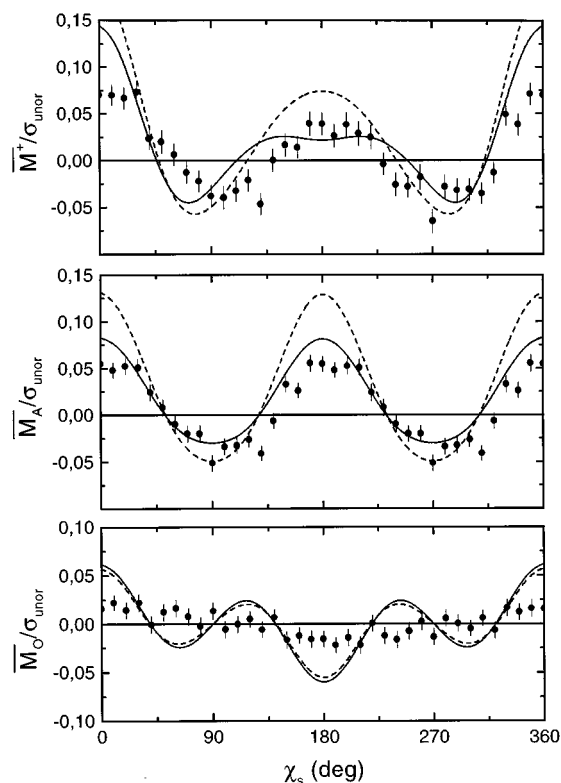
FIG. 3. Same azimuthal distribution as in Fig. 2, but for the oriented state mixture focused at $U_0=\pm 10$ kV.

that mixtures with different rotational state populations are present in the scattering region for different U_0. When U_0 is changed from ± 4 kV to ± 10 kV the calculated mean degree of orientation is reduced from 0.43 to 0.17 and the beam intensity increases by about a factor of 2. That the measured distributions of Figs. 2(a) and 3(a) are fairly similar can be considered accidental; this is not expected for azimuthal distributions at other polar angles. The corresponding diffraction patterns in the parallel geometry changed quite dramatically when the state mixture was changed [12].

By applying the IAM to oriented molecules [7,13], we have also calculated the azimuthal scattering distributions. The population fractions of the various molecular rotational states focused into the scattering region were determined by calculation of the Boltzmann state distribution (for a single rotational temperature $T_{rot}=25$ K corresponding to the nozzle expansion conditions) and the transmission and focusing of the hexapole using the Stark effect and neglecting nuclear hyperfine coupling (see also Ref. [12]). With these population fractions and the molecular structure data for CH_3Cl [17] the mean interference terms $\bar{M}^+$, $\bar{M}_A$, and $\bar{M}_O$ were calculated without vibrational damping (see Ref. [13]), but taking the experimental angular resolution into account. The numerical results are also shown in Figs. 2 and 3 for comparison to the experimental data. The dashed curves represent the case when only the linear Stark effect is taken into account for the motion of the molecules in the hexapole field, as in our previous calculations [12,13].

In order to improve the modeling, we have now additionally included focusing by the quadratic Stark effect, employing the approximate formulas for the peak shift with respect to

to U_0 as described recently by Ohoyama *et al.* [18]. The inclusion of the quadratic Stark effect leads to a substantial change of the relative weight of some focused states. The resulting scattering distributions for such modified state mixtures are plotted as full drawn lines in Figs. 2 and 3. The agreement between model and experiment for $\bar{M}^+/\sigma_{\mathrm{unor}}$ is improved at both $U_0 = \pm 4$ kV and $U_0 = \pm 10$ kV when the second-order Stark effect is also included, since the alignmentlike contributions are changed considerably. However, both calculations fail to reproduce the observed orientation-like interference parts of Figs. 2(c) and 3(c) with sufficient precision. The theoretically predicted phase change of the oscillations when increasing U_0 from ± 4 kV to ± 10 kV is not seen clearly in the data.

Closer inspection of the numerical results shows that at $U_0 = \pm 4$ kV the $|111\rangle$, $|212\rangle$, and $|221\rangle$ states together account for more than 1/3 of the total state population. When the quadratic Stark effect is included, the relative weight of the $|111\rangle$ state increases; it then accounts for 0.30, whereas the $|212\rangle$ and $|221\rangle$ states contribute only a few percent. Thus, inclusion of the quadratic Stark effect leads to a more $|111\rangle$-like diffraction pattern, as observed experimentally. Previously, the comparison for the parallel geometry has also shown that the influence of the $|111\rangle$ state was underestimated in the linear Stark effect model at $U_0 = \pm 4$ kV [12]. In the calculations for $U_0 = \pm 10$ kV many states contribute, with the largest weight for the $|211\rangle$ and $|312\rangle$ states and negligible population of $|111\rangle$. Inclusion of the second-order Stark effect changes the relative weights to some degree. The shift with respect to U_0 due to the quadratic Stark effect is negative for the $|211\rangle$ state, in contrast to most others (see Ref. [18]), explaining most of the differences of the two curves.

In summary, the comparison of model calculations with our experimental data shows that the diffraction patterns depend very sensitively on the state mixtures present in the scattering region. Further effects that could lead to a possible change of the relative state populations in the scattering region are nuclear hyperfine coupling, nonadiabatic transitions between rotational states, deviations from the ideal hexapole field configuration due to cylindrical rods, higher-order Stark effects, and an incomplete switching off of orientation or alignment, as discussed, in part, previously [13]. More elaborate trajectory calculations modeling the hexapole focusing by taking the exact Stark interactions and cylindrical rod configurations into account are currently being developed by Anderson [19].

We have also measured the azimuthal scattering distributions at $\vartheta = 11.0°$, which are, however, less pronounced. Since the measurements discussed here are very time consuming, it will be advantageous to record the diffraction pattern with a two-dimensional detection scheme in the future. The implications of a two-dimensional analysis of the electron diffraction pattern from oriented molecules for molecular structure analysis have been discussed elsewhere [20]. The modeling of the experimentally observed scattering distributions carried out here and in Refs. [12, 13] for the azimuthal and polar distributions has revealed the crucial importance of the calculated state populations and has not given any indication so far that the IAM description is not sufficiently precise for this application.

[1] R. A. Bonham and M. Fink, *High Energy Electron Scattering* (Van Nostrand Reinhold, New York, 1974).

[2] E. A. V. Ebsworth, D. W. H. Rankin, and S. Cradock, in *Structural Methods in Inorganic Chemistry* (Blackwell Scientific Publications, Oxford, 1987), Chap. 8.

[3] *Stereochemical Applications of Gas Phase Electron Diffraction,* edited by I. Hargittai and M. Hargittai (VCH, Weinheim, 1988), Vols. A and B.

[4] R. J. Allan and A. S. Dickinson, J. Phys. B **13**, 3493 (1980).

[5] M. Fink, A. W. Ross, and R. J. Fink, Z. Phys. D **11**, 231 (1989).

[6] A. Mihill and M. Fink, Z. Phys. D **14**, 77 (1989).

[7] D. A. Kohl and E. J. Shipsey, Z. Phys. D **24**, 33 (1992).

[8] D. A. Kohl and E. J. Shipsey, Z. Phys. D **24**, 39 (1992).

[9] J. C. Williamson and A. H. Zewail, J. Phys. Chem. **98**, 2766 (1994).

[10] C. Ostrawsky, K. Blum, and C. Gillan, J. Phys. B **28**, 2269 (1995).

[11] M. Volkmer *et al.*, Phys. Rev. Lett. **68**, 2289 (1992).

[12] N. Böwering *et al.*, Z. Phys. D **30**, 117 (1994).

[13] M. Volkmer *et al.*, Phys. Rev. A **53**, 1457 (1996).

[14] T. Kasai *et al.*, Phys. Rev. Lett. **70**, 3864 (1993).

[15] C. G . Aitken, D. A. Blunt, and P. W. Harland, Int. J. Mass Spectrom. Ion Processes **149/150**, 279 (1995).

[16] J. Bulthuis, J. B. Milan, M. H. M. Janssen, and S. Stolte, J. Chem. Phys. **94**, 7181 (1991).

[17] L. S. Bartell and L. O. Brockway, J. Chem. Phys. **23**, 1860 (1955).

[18] H. Ohoyama, T. Ogawa, and T. Kasai, J. Phys. Chem. **99**, 13 606 (1995).

[19] R. W. Anderson, J. Phys. Chem. (to be published).

[20] N. Böwering *et al.*, J. Mol. Struct. **348**, 49 (1995).